

Atomistic description of oxide formation on metal surfaces: the example of ruthenium

Karsten Reuter ^{a,*}, Catherine Stampfl ^{a,b}, M. Verónica Ganduglia-Pirovano ^a,
Matthias Scheffler ^a

^a Fritz-Haber-Institut der Max-Planck-Gesellschaft, Faradayweg 4-6, D-14195 Berlin, Germany

^b Northwestern University, 2145 Sheridan Road, Evanston, IL 60208, USA

Received 6 August 2001; in final form 17 December 2001

Abstract

The microscopic process of the formation of oxides on metal surfaces is barely known or understood. Using density-functional theory we studied the oxidation of Ru(0001): from the initial oxygen adsorption, subsequent O incorporation into the metal, aggregation of sub-surface islands, to the transition to the oxide film. Along the atomistic pathway several metastable precursor configurations are identified. It is argued that their properties and the metastabilities in the surface-oxide formation process will have important consequences for the discernment and molecular modeling of catalysis. © 2002 Elsevier Science B.V. All rights reserved.

1. Introduction

Under *realistic* conditions a surface is in contact with a rich environment, and the interaction with the atoms and molecules of the surrounding phase can induce significant material changes, exemplified by the corrosion of metal surfaces. Although such oxidized surfaces are an everyday phenomenon in our oxygen-rich atmosphere, the knowledge and understanding about the atomistic mechanisms involved in the process of oxide formation is very shallow. A better understanding is, for example, important for catalysis research, where the

often long induction periods (from seconds to days), required to achieve efficient performance, indicate that the native catalyst structure is significantly changed when placed in the realistic environment [1].

That the active material may actually not be the originally introduced metal, but an oxide (or surface-oxide) phase has recently been discussed in several studies (see e.g. [2] and references therein). For example, Rolison et al. [3] showed that the industrial Pt–Ru catalysts used for the oxidation of methanol are not simply bimetallic alloys, but contain hydrous Ru oxide, the presence of which is an essential prerequisite to achieve the desired turnover rates. Similarly, a high activity towards CO oxidation was reported for heavily O dosed Ru(0001) [4,5], which was subsequently related to

* Corresponding author. Fax: +49-3084134701.

E-mail address: reuter@fhi-berlin.mpg.de (K. Reuter).

the formation of crystalline $\text{RuO}_2(110)$ domains on the surface [6]. In fact, it has been known for some time, that the catalytic activity of the clean Ru metal surface, as studied under ultra-high vacuum conditions, is much lower than that of Ru under realistic oxygen pressure conditions (see e.g. [4,7]).

In this Letter we discuss the changes that occur at the (0001) surface of ruthenium when held in an oxygen atmosphere. In view of the above-mentioned experimental studies, the characterization of this surface is indeed unique: That is, the initial state, i.e. the clean metal surface, as well as several adsorbate geometries, and the final state, i.e., the RuO_2 oxide, have all been convincingly identified (on the atomic level) [6,8]. However, the *pathway* of the final transition towards the oxide is so far unknown and probably difficult to identify experimentally. In the present work, on the basis of extensive density-functional theory (DFT) calculations, we identify this pathway as well as three metastable configurations along the way that should be observable in carefully directed experiments. Although we discuss Ru, the reasoning for this choice given above, we note that other transition metals are expected to exhibit a similar behavior, e.g., the existence of metastable surface-localized oxide-like configurations that are unknown for bulk systems. Furthermore, the likely lively dynamics between these metastable configurations will affect the surface chemical properties under realistic conditions, and hence any catalytic reactions taking place over them. Clearly, before the dynamics can be studied, it is first necessary to discover and analyze these metastable states, and this is what is done in the present Letter.

2. Theory

Our DFT calculations employ the generalized gradient approximation for the exchange-correlation functional [9]. The Kohn–Sham equations are solved using the full-potential linearized augmented plane wave (FP-LAPW) method [10,11], modeling the metal surface by a six layer slab for $\theta \leq 2$ monolayers (ML) and a 10 layer slab for higher coverages. Adsorption is on both sides,

fully relaxing the outermost two (three) Ru layers of the six (10) layer slabs, as well as the position of all O atoms. The high accuracy of the used FP-LAPW basis set [12] was already described for the on-surface O adsorption regime [13] and is characterized by a ± 30 meV (± 50 meV) numerical uncertainty, when comparing relative binding energies in geometries containing an equal (unequal) amount of O.

3. Results

3.1. Initial incorporation and sub-surface island formation

Initial O adsorption on the bare Ru(0001) surface results in the formation of four ordered phases, in which with increasing coverage O consecutively fills the four available hcp sites inside a (2×2) unit mesh [8,14]. As shown in Fig. 1, the binding energy per O atom decreases markedly during this coverage sequence, reflecting the repulsive interaction between the electronegative

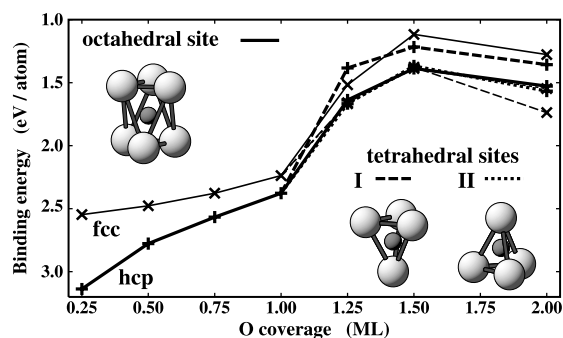


Fig. 1. Binding energies per O atom, $E(\theta)$, with respect to $1/2 \text{ O}_2$. Coverages with $\theta < 1$ ML correspond to pure on-surface adsorption (hcp or fcc site). For $\theta > 1$ ML an $\text{O}(1 \times 1)$ arrangement is always present at the surface, while the remaining O is located in either the octahedral or one of the two tetrahedral sites between the first and second substrate layer. The insets show the local atomic coordination of each of these sub-surface sites (Ru = light, big spheres, O = dark, small spheres). From the six possible structures at each coverage, the three with the on-surface O in hcp (fcc) sites are drawn with thicker (thinner) lines. Note, that the hcp/tetra-II and fcc/tetra-II geometries are almost equally stable, which is why only the hcp/tetra-II line is plotted.

adsorbates [14]. We notice in passing that this decreasing trend is found for O adsorption on the basal surface of the late 4d transition metals from Ru to Ag [14–16], but is contrasted by the increase in binding energy found for O on Al(111) [17], there leading to the formation of small close-packed O islands at sub-monolayer coverages [18].

Earlier calculations for O/Ru(0001) [19] had already shown that oxygen will first occupy on-surface hcp sites and only when the monolayer is complete the additional oxygen goes sub-surface. Recent experiments by Böttcher and Niehus [20] confirmed this prediction. Increasing the oxygen coverage beyond 1 ML, we find that this additional O resides below the top Ru layer, i.e. it is energetically unfavorable to diffuse into the bulk. In analogy to the on-surface case, we employ (2×2) unit cells, in which consecutively more and more sub-surface O is placed, to study the O incorporation for coverages $1 \text{ ML} < \theta \leq 2 \text{ ML}$. Three different highly coordinated sub-surface sites are available, and all of them were studied: one octahedral site (sixfold Ru coordination) and two tetrahedral sites (fourfold Ru coordination), the local atomic surrounding of which is shown in Fig. 1. The octahedral site is the site directly below the on-surface fcc site (henceforth referred to as octa), while one of the two tetrahedral sites (tetra-I) is the site directly below the on-surface hcp site. Thirdly, oxygen can also occupy the site right below a surface Ru atom (tetra-II). Combining the O(1×1) adlayer in either hcp or fcc sites with the three available sub-surface sites results in six possible geometries at each coverage, some of which were initially investigated in [21]. The corresponding average binding energies per O, $E(\theta)$, with respect to $1/2 \text{ O}_2$ are displayed in Fig. 1 which shows that all structures are exothermic with respect to clean Ru(0001) and molecular oxygen, and should thus be able to form. The energies for higher coverage are much lower than those for the pure on-surface adsorption for $\theta < 1 \text{ ML}$, indicating that the now additionally occupied sub-surface sites are energetically considerably less favorable. Interestingly, $E(\theta)$ does not decrease monotonically with coverage, but the most stable configuration is obtained for a 2 ML geometry with the on-surface O in fcc and the sub-surface O

in tetra-I sites, cf. Fig. 1. Consequently, it will be energetically more favorable to distribute the excess oxygen for coverages with $\theta > 1 \text{ ML}$ in form of locally close-packed sub-surface islands, gaining $E(2 \text{ ML, fcc/tetra-I})$ per oxygen atom, rather than forming more dilute sub-surface phases, where then only the lower $E(1 \text{ ML} < \theta \leq 2 \text{ ML})$ is freed. Thus, contrary to the chemisorption regime ($\theta < 1 \text{ ML}$), where the oxygen adatoms prefer to stay as far away from each other as possible, we find that sub-surface O prefers to form islands with a local (1×1) periodicity. In the following we will therefore restrict our discussion to the periodic core of such islands, which can be addressed within the framework of our periodic boundary conditions.

3.2. Trilayer formation, registry shift and decoupling

At a first glance it appears that kinetics will hinder the formation of a geometry with one oxygen in the on-surface fcc site and another one in the sub-surface tetra-I site: This geometry seems to imply that all initially adsorbed adatoms, which for coverages up to 1 ML sit in on-surface hcp sites, have to change their positions. Yet, a deeper analysis predicts the following scenario: The full on-surface oxygen adlayer (hcp sites) is followed by close-packed sub-surface islands with oxygen e.g. in octa sites, and this combination is found to be unstable against a registry shift of the whole O–Ru–O trilayer along the $[\bar{1}\bar{1}2]$ direction as shown in Fig. 2. During this shift, the electronic as well as the geometric structure within the trilayer are found to remain virtually unchanged, reflecting its strongly bound, sub-unit like nature. The substantial binding energy gain of 0.2 eV per O atom upon this displacement is due to an improved bonding between the sub-surface oxygens and the topmost Ru atoms of the underlying metal, i.e. the second Ru layer. In particular, on-surface oxygen atoms are located in fcc and the sub-surface O in tetra-I sites (see Fig. 1). The only difference of this structure compared to the originally tested fcc/tetra-I geometry is that the O–Ru–O trilayer, as a whole, is rotated by 60° with respect to the metal below, i.e., both the internal trilayer geometry as

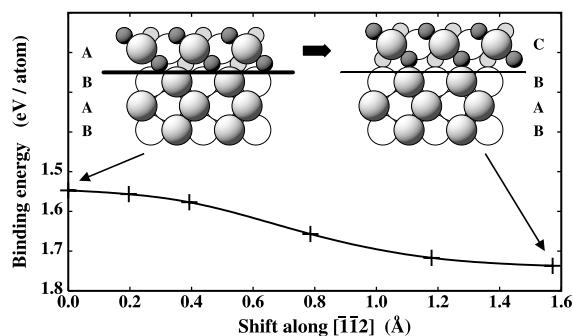


Fig. 2. Side views of the hcp/octahedral and fcc/tetrahedral-I geometries of the O–Ru–O trilayer over the Ru(0001) substrate (Ru = light, big spheres, O = dark, small spheres, atoms not lying inside the plane itself are white). Lower half: binding energy per O along the trilayer shift indicated by the arrow.

well as the coordination of the sub-surface oxygen with respect to its Ru neighbors are the same. Just the first Ru layer finds itself in a stacking-fault geometry with respect to the remaining Ru substrate.

The coupling of this trilayer to the underlying metal is rather weak, and now only via the sub-surface O and the second Ru layer since the first metal layer distance, $d_{1,2}(\text{Ru})$, is notably expanded by 62% compared to the Ru bulk value. The reduced binding is reflected by the fact that to completely lift off the trilayer it costs only 1.4 eV per (1×1) cell, in comparison to 2.7 eV as required to lift off a Ru layer from a clean Ru(0001) surface. Hence, we find a significant destabilization of the metal surface due to the formation of the O–Ru–O trilayer, which is more strongly bound in itself than to the remaining metal substrate. Of course, in reality the adsorption process starts with finite-size islands of sub-surface oxygen, and the shift may be expected to happen at step edges.

It is the combination of the internal trilayer geometry and the trilayer–metal coupling that explains the pronounced energetic preference for the fcc/tetra-I structure compared to all other tested geometries, cf. Fig. 1. Only the combinations hcp/octa and fcc/tetra-I lead to a trilayer geometry, in which each Ru atom is located inside an octahedron formed by three on-surface and three sub-surface oxygens as depicted in Fig. 4, left middle panel. And as explained above, the latter has a

more favorable bonding of the sub-surface O to the second Ru layer. This sixfold O coordination, also found in the RuO_2 bulk oxide, offers a preferred bonding situation compared to the fourfold O coordination, present in the two geometries with the sub-surface O in tetra-II positions. In the two remaining combinations, fcc/octa and hcp/tetra-I, the electronegative on- and sub-surface oxygens sit directly on top of each other, rendering these structures energetically less stable due to electrostatic repulsion [22].

Although the sixfold geometry of Ru in the trilayer has already some resemblance to the bulk oxide, the geometry is still distinctly different to that of the experimentally observed $\text{RuO}_2(110)$. We therefore considered the incorporation of even more oxygen into the system and we find we are led quite naturally, via a rather novel mechanism, to $\text{RuO}_2(110)$. In addition to the hitherto considered $\text{O}(1 \times 1)$ on- and sub-surface O structures we placed another ML of O in sites between the second and third substrate layers (the total O coverage is now 3 ML). With the two possible on-surface and three possible sub-surface sites (for which we now have two to consider), this gives a total of 18 trial geometries. Surprisingly, the most stable structure corresponds to none of these, but to one where the additional oxygen is also located between the first and second Ru layers, where already another full layer of oxygen has found its place (cf. Fig. 3). Due to the additional sub-surface O, the O–Ru–O trilayer becomes almost completely decoupled from the underlying Ru metal, as indicated by the significant first metal layer expansion of 116% and the essentially separated electron density, also displayed in Fig. 3.

3.3. Continued oxidation and transition to the oxide structure

Considering the Ru substrate below the trilayer in more detail, we find its electronic and geometric structure to be very similar to that of a $\text{O}(1 \times 1)$ covered Ru(0001) surface with 1 ML O in hcp sites. The trilayer on top has apparently only negligible influence on the underlying metal. From this we deduce that the continued interaction of

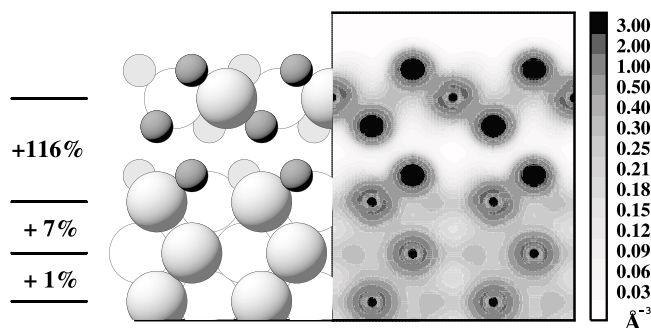


Fig. 3. Side view of the most stable geometry with 3.0 ML O. The on-surface O sits in fcc sites, while the sub-surface O occupies both the tetrahedral-I and -II sites between the first and second substrate layer. The left half of the figure shows the schematic geometry together with the relative layer expansions compared to the bulk distance and the right half the calculated electron density.

O with the Ru(0001) surface will proceed in a similar fashion as before, i.e., the coverage sequence $3 \text{ ML} < \theta \leq 4 \text{ ML}$ will lead to the formation of a second O–Ru–O trilayer, which in turn

will become decoupled from the deeper metal substrate by the fifth ML of oxygen, and so on. This way a stack of loosely coupled trilayers will successively be formed.

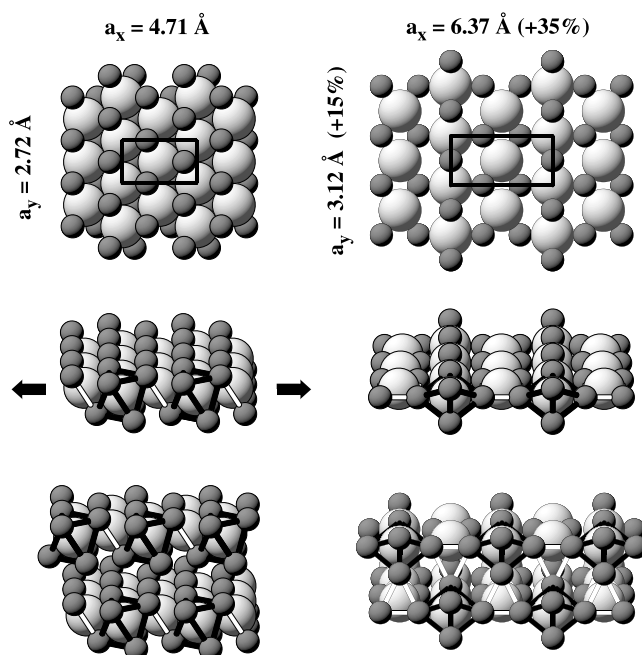


Fig. 4. Atomic geometries of the O–Ru–O trilayer (left-hand side) and the $\text{RuO}_2(110)$ structure (right-hand side). Top panel: top view, indicating the relative sizes of the surface unit cells. Middle panel: perspective view. The rutile structure is achieved by simply expanding the trilayer, while keeping the length of the drawn O–O bonds (white and black lines) rigid. This way, an alternating sequence of fully coordinated Ru atoms (inside the tilted O octahedra, black bonds) and coordinatively unsaturated (cus) Ru atoms (surrounded by only four O atoms, white bonds) is created. Bottom panel: coupling of two trilayers vs. that of rutile layers. Whereas the self-contained trilayers hardly bind, new bonds can be formed in the $\text{RuO}_2(110)$ structure. The bridging O atoms of the full octahedra (black bonds) form the apex atoms of the new octahedra (white bonds) around the former cus Ru atoms. Note, that the ‘bonds’ drawn do not refer to chemical bonds, but are merely used to guide the eye.

Fig. 4 compares the geometry of the experimentally observed (110) orientation of RuO_2 patches (right) [6] with our trilayer (left). It can be noticed that the latter can be transformed into $\text{RuO}_2(110)$ by a simple accordion-like lateral expansion of the trilayer, cf. Fig. 4. With this expansion the self-contained trilayer, offering the preferred sixfold O coordination to every Ru atom, unfolds into a more open geometry, in which every second Ru atom is now only fourfold O coordinated. It is precisely these coordinatively unsaturated (cus) metal atoms that eventually lead to a stabilization of the rutile structure for higher film thicknesses as explained as follows: Whereas two trilayers are found to bind only weakly to each other, after the accordion-like expansion, new bonds between the bridging O atoms of the octahedra and the cus metal atoms are formed (cf. Fig. 4). In contrast to the loose stacking of trilayers, the binding energy per O atom in a rutile film increases therefore gradually with the number of layers, rendering the latter energetically more favorable after a critical film thickness is exceeded. This thickness is found to correspond to 5 ML of oxygen: While one trilayer is by 0.15 eV per O atom more stable than its rutile structured counterpart, this energetic sequence is already reversed for the two trilayer case. For thick films, this difference finally approaches a value of 0.6 eV per O atom, by which the bulk rutile RuO_2 oxide is more stable. Thus, we estimate that the phase transition into a $\text{RuO}_2(110)$ oxide film will only start after two or more O–Ru–O trilayers have formed. Together with the terminal O layer, saturating the substrate, this amounts to a local oxygen coverage of 5 ML. The thus formed oxide overlayer is incommensurate, but aligned to $\text{Ru}(0001)$, in agreement with the STM study of Over et al. [6].

4. Summary

In conclusion, we described an atomistic mechanism leading to $\text{RuO}_2(110)$ oxide patches on $\text{Ru}(0001)$. After the on-surface oxygen adlayer is completed, we identified through our DFT study

three metastable precursor configurations that define the pathway towards the formation of $\text{RuO}_2(110)$ [22]:

- (i) Oxygen adsorption beyond 1.5 ML gives rise to close-packed sub-surface oxygen islands between the first and second Ru layer. This is a rather stable O–Ru–O trilayer.
- (ii) When the extension of this sub-surface island becomes large, a shift of the trilayer is predicted, giving rise to a stacking-fault geometry of the top Ru layer with respect to the remaining metal substrate.
- (iii) Continuing the oxidation results in the geometry shown in Fig. 3. Then, a successive formation of trilayers occurs, which will finally ‘unfold’ into the rutile bulk oxide structure after a critical thickness is exceeded.

The various structures are found to be very close in energy, thus, depending on the temperature, and in particular at the higher temperatures and under the conditions of catalysis, it is expected that this surface will indeed be in a dynamic ‘living’ state. This situation will markedly influence catalytic reactions that are performed over such a surface, and it also dictates that it will be crucial to take the dynamics into account when one attempts molecular modeling of catalysis. Finally we mention that preliminary calculations for O/Rh(111) [23] and O/Ag(111) [24], as well as published results for sub-surface O/Al(111) [17], indicate that the various mechanisms identified here may be more general, namely, the tendency for the formation of sub-surface O islands which destabilize the metal surface and represent metastable precursors for the phase transition to a surface-oxide.

Acknowledgements

This work was partially supported by the Deutsche Forschungsgemeinschaft (Schwerpunkt ‘Katalyse’).

References

- [1] G. Ertl, H. Knözinger, J. Weitkamp (Eds.), Handbook on Heterogeneous Catalysis, Wiley, New York, 1997.

- [2] C. Stampfl et al., Surf. Sci. 500 (2001) xxx. Preprint: available from <http://www.fhi-berlin.mpg.de/th/publications/Surf.-Sci.-500-2001.pdf>.
- [3] D.R. Rolison et al., Langmuir 15 (1999) 774.
- [4] A. Böttcher et al., J. Phys. Chem. B 101 (1997) 11185.
- [5] A. Böttcher, H. Conrad, H. Niehus, Surf. Sci. 452 (2000) 125.
- [6] H. Over et al., Science 287 (2000) 1474.
- [7] T.E. Madey, H.A. Engelhardt, D. Menzel, Surf. Sci. 48 (1975) 304.
- [8] D. Menzel, Surf. Rev. Lett. 6 (1999) 835.
- [9] J.P. Perdew, K. Burke, M. Ernzerhof, Phys. Rev. Lett. 77 (1996) 3865.
- [10] P. Blaha et al., Comp. Phys. Commun. 59 (1990) 399.
- [11] M. Petersen et al., Comp. Phys. Commun. 126 (2000) 294.
- [12] FP-LAPW basis set: $R_{MT}^{Ru} = 1.21 \text{ \AA}$, $R_{MT}^O = 0.69 \text{ \AA}$, $E_{max}^{wf} = 17 \text{ Ry}$, $E_{max}^{pot} = 169 \text{ Ry}$, $l_{max}^{wf} = 12$, $l_{max}^{pot} = 4$, 19 \mathbf{k} -points in the irreducible part of the (1×1) BZ.
- [13] S. Lizzit et al., Phys. Rev. B 63 (2001) 205419.
- [14] C. Stampfl, M. Scheffler, Phys. Rev. B 54 (1996) 2868.
- [15] M.V. Ganduglia-Pirovano, M. Scheffler, Phys. Rev. B 59 (1999) 15533.
- [16] M. Todorova et al., Phys. Rev. Lett. (submitted).
- [17] A. Kiejna, B.I. Lundqvist, Phys. Rev. B 63 (2001) 85405.
- [18] H. Brune et al., Phys. Rev. Lett. 68 (1992) 624.
- [19] C. Stampfl et al., Phys. Rev. Lett. 77 (1996) 3371.
- [20] A. Böttcher, H. Niehus, J. Chem. Phys. 110 (1999) 3186.
- [21] C. Stampfl et al., Appl. Phys. A 69 (1999) 471.
- [22] K. Reuter et al., Phys. Rev. B, to be published.
- [23] M.V. Ganduglia-Pirovano, K. Reuter, M. Scheffler, Phys. Rev. B, submitted.
- [24] W. Li, C. Stampfl, M. Scheffler, Phys. Rev. B 65 (2002), to be published.